

Voltage sensor interaction site for selective small molecule inhibitors of voltage-gated sodium channels

Ken McCormack^{a,1}, Sonia Santos^a, Mark L. Chapman^a, Douglas S. Krafte^a, Brian E. Marron^a, Christopher W. West^a, Michael J. Krambis^a, Brett M. Antonio^a, Shannon G. Zellmer^a, David Printzenhoff^a, Karen M. Padilla^a, Zhixin Lin^a, P. Kay Wagoner^{a,2}, Nigel A. Swain^b, Paul A. Stuppel^{c,3}, Marcel de Groot^c, Richard P. Butt^b, and Neil A. Castle^{a,4}

^aIcagen Inc. (currently Neusentis, Research Unit of Pfizer Inc.), Durham, NC 27703; ^bNeusentis, Research Unit of Pfizer Inc., Cambridge CB21 6GS, United Kingdom; and ^cPfizer Ltd., Sandwich, Kent CT13 9NJ, United Kingdom

Edited by Kurt G. Beam, University of Colorado at Denver, Aurora, CO, and approved June 5, 2013 (received for review December 10, 2012)

Voltage-gated sodium (Na_v) channels play a fundamental role in the generation and propagation of electrical impulses in excitable cells. Here we describe two unique structurally related nanomolar potent small molecule Na_v channel inhibitors that exhibit up to 1,000-fold selectivity for human $\text{Na}_v1.3/\text{Na}_v1.1$ (ICA-121431, IC_{50} , 19 nM) or $\text{Na}_v1.7$ (PF-04856264, IC_{50} , 28 nM) vs. other TTX-sensitive or resistant (i.e., $\text{Na}_v1.5$) sodium channels. Using both chimeras and single point mutations, we demonstrate that this unique class of sodium channel inhibitor interacts with the S1–S4 voltage sensor segment of homologous Domain 4. Amino acid residues in the “extracellular” facing regions of the S2 and S3 transmembrane segments of $\text{Na}_v1.3$ and $\text{Na}_v1.7$ seem to be major determinants of Na_v subtype selectivity and to confer differences in species sensitivity to these inhibitors. The unique interaction region on the Domain 4 voltage sensor segment is distinct from the structural domains forming the channel pore, as well as previously characterized interaction sites for other small molecule inhibitors, including local anesthetics and TTX. However, this interaction region does include at least one amino acid residue [E1559 ($\text{Na}_v1.3$)/D1586 ($\text{Na}_v1.7$)] that is important for Site 3 α -scorpion and anemone polypeptide toxin modulators of Na_v channel inactivation. The present study provides a potential framework for identifying subtype selective small molecule sodium channel inhibitors targeting interaction sites away from the pore region.

Voltage-gated sodium (Na_v) channels play an important role in the generation and propagation of electrical signals in excitable cells (1–3). Eukaryotic Na_v channels are heteromeric membrane proteins composed of a pore-forming α -subunit and auxiliary β -subunits (3, 4). The mammalian genome encodes nine distinct α ($\text{Na}_v1.1$ – 1.9) and four β subunits (3). The α -subunit comprises four homologous domains (D1–D4), each of which contains six transmembrane segments (S1–S6) (3–5). The S5 and S6 segments form the central pore separated by the SS1 and SS2 segments, which form the ion selectivity filter at its extracellular end. The S1 to S4 segments form the voltage sensor (3–5).

Both naturally occurring and synthetic pharmacological modulators of sodium channel have been identified (6–11), and for many, their site of interaction has been defined. For example, the marine toxin TTX inhibits several Na_v subtypes by interacting with amino acid residues within the SS1–SS2 segments that define the outer pore of the channel (12, 13). In contrast, the polypeptide α - and β -scorpion venom toxins, which enhance sodium channel activation or delay inactivation, and spider venom toxin sodium channel inhibitors like Protx II interact with specific residues on the S1–S4 voltage sensor regions within homologous Domain 2 (i.e., β -scorpion toxins, Protx II) or Domain 4 (i.e., α -scorpion toxins, anemone toxins) of the channel (8, 14–18). Many synthetic small molecule inhibitors of Na_v channels, including local anesthetic, antiepileptic, and antiarrhythmic agents, are believed to interact with amino acid residues within the S6 segment in Domain 4, which forms part of the pore lining and is structurally highly conserved across subclasses of mammalian Na_v channels (11, 19–22). This structural homology probably

accounts for many clinically used local anesthetics and related antiepileptic and antiarrhythmic inhibitors, exhibiting little or no selectivity across the nine subtypes of mammalian Na_v channels (23). In the clinic this absence of subtype selectivity can result in toxicities associated with unwanted interactions with off-target Na_v channels (e.g., cardiac toxicity due to inhibition of cardiac $\text{Na}_v1.5$ channels) (24, 25). Therefore, because of their importance in normal physiology and pathophysiology, identification of selective pharmacological modulators of Na_v channels is of considerable interest to the scientific and medical communities (9, 23, 26–29). For example, in addition to the therapeutic utility of sodium channel inhibitors described above, there has been recent interest in potentially targeting inhibition of specific Na_v channel subtypes (i.e., $\text{Na}_v1.7$, $\text{Na}_v1.8$, and $\text{Na}_v1.3$) for the treatment of pain (9, 30–32).

The present study describes the characterization of a class of subtype selective sodium channel inhibitor that interacts with a unique site on the voltage sensor region of homologous Domain 4. This inhibitory interaction site differs from previously reported inhibitor binding sites for TTX and local anesthetic-like modulators (11, 12).

Significance

Voltage-gated sodium (Na_v) channels contribute to physiological and pathophysiological electrical signaling in nerve and muscle cells. Because Na_v channel isoforms exhibit tissue-specific expression, subtype selective modulation of this channel family provides important drug development opportunities. However, most available Na_v channel modulators are unable to distinguish between Na_v channel subtypes, which limits their therapeutic utility because of cardiac or nervous system toxicity. This study describes a new class of subtype selective Na_v channel inhibitors that interact with a region of the channel that controls voltage sensitivity. This interaction site may enable development of selective therapeutic interventions with reduced potential for toxicity.

Author contributions: K.M., M.L.C., and N.A.C. designed research; K.M., S.S., M.L.C., M.J.K., B.M.A., S.G.Z., D.P., and Z.L. performed research; K.M., S.S., B.E.M., C.W.W., K.M.P., Z.L., P.K.W., N.A.S., P.A.S., M.d.G., and R.P.B. contributed new reagents/analytic tools; K.M., S.S., M.L.C., M.J.K., B.M.A., S.G.Z., D.P., Z.L., and N.A.C. analyzed data; and K.M., D.S.K., and N.A.C. wrote the paper.

The authors declare no conflict of interest.

This article is a PNAS Direct Submission.

¹Present address: Arisan Therapeutics, Inc., San Diego, CA 92121.

²Present address: P. Kay Wagoner Discovery and Development Consulting, Chapel Hill, NC 27516.

³Present address: Walter and Eliza Hall Institute of Medical Research Biotechnology Centre, Bundoora, VIC 3086, Australia.

⁴To whom correspondence should be addressed. E-mail: neil.castle@pfizer.com.

This article contains supporting information online at www.pnas.org/lookup/suppl/doi:10.1073/pnas.1220844110/-DCSupplemental.

Results

Characterization of a Subtype Selective Inhibitor of Human $\text{Na}_v1.3$ Channels. During a Na_v channel inhibitor drug candidate discovery program, a previously uncharacterized agent, ICA-121431 [2,2-diphenyl-*N*-(4-(*N*-thiazol-2-ylsulfamoyl)phenyl) acetamide] was found to inhibit human TTX-sensitive $\text{Na}_v1.3$ sodium channels stably expressed in HEK-293 cells (Fig. 1A). As with many known voltage-dependent sodium channel inhibitors, inhibition of human $\text{Na}_v1.3$ by ICA-121431 was found to be dependent on channel gating state. When $\text{Na}_v1.3$ currents were elicited by 20-ms depolarizing voltage steps from -120 mV, at which channels are predominantly in a resting closed state, ICA-121431 had a negligible effect on current amplitude at $1 \mu\text{M}$ (Fig. 1B). In contrast, when a test pulse was preceded by an 8-s conditioning voltage step to a membrane potential that resulted in approximately half of the channels being in an inactivated state, $1 \mu\text{M}$ ICA-121431 produced $92\% \pm 4\%$ ($n = 4$) reduction in current amplitude (Fig. 1B). A preferential interaction with inactivated $\text{Na}_v1.3$ channels was further supported by the finding that ICA-121431 elicited a concentration-dependent hyperpolarizing shift in the voltage dependence of inactivation (Fig. 1C).

Although ICA-121431 produced negligible inhibition when test pulses were applied from a -120 mV holding potential at a relatively low stimulation frequency (i.e., 0.05 Hz), cumulative (or use-dependent) inhibition became evident when stimulation frequency was increased to 10 Hz (Fig. 1D). This use-dependent inhibition of

$\text{Na}_v1.3$ by ICA-121431 clearly differs from the absence of frequency-dependent inhibition in the presence of TTX (Fig. 1D).

Although state- and/or frequency-dependent inhibition is a relatively common characteristic of small molecule voltage-gated sodium channel inhibitors (33), a more unique finding was the marked subtype selectivity exhibited by ICA-121431. Fig. 1E shows that in contrast to $\text{Na}_v1.3$, $1 \mu\text{M}$ ICA-121431 produced little or no inhibition of human $\text{Na}_v1.7$ or $\text{Na}_v1.5$ currents. Selective inhibition of $\text{Na}_v1.3$ by ICA-121431 is further illustrated in Fig. 1F, which shows the concentration dependence of inhibition of human $\text{Na}_v1.3$, $\text{Na}_v1.5$, and $\text{Na}_v1.7$ measured on the IonWorks Quattro automated electrophysiology using a 500-ms conditioning pulse to 0 mV to promote availability of the inactivated state. Under these conditions, the IC_{50} for ICA-121431 inhibition of $\text{Na}_v1.3$ was 19 ± 5 nM ($n = 6$), compared with $>10 \mu\text{M}$ for both human $\text{Na}_v1.5$ and $\text{Na}_v1.7$. When additional Na_v channel subtypes were examined, the selectivity profile of ICA-121431 was found to cover a spectrum of inhibitor potencies, with human $\text{Na}_v1.3$ and $\text{Na}_v1.1$ being the most sensitive to inhibition (IC_{50} s <20 nM), $\text{Na}_v1.2$ having an intermediate sensitivity (IC_{50} 240 nM), whereas $\text{Na}_v1.4$, $\text{Na}_v1.5$, $\text{Na}_v1.6$, $\text{Na}_v1.7$, and $\text{Na}_v1.8$ were relatively insensitive to inhibition (IC_{50} s $>10 \mu\text{M}$) (Fig. S1 and Table S1).

ICA-121431 Interacts with Homologous Domain 4 of $\text{Na}_v1.3$. Given the potency and selectivity of ICA-121431, we were interested in further understanding its interaction with human $\text{Na}_v1.3$ and the

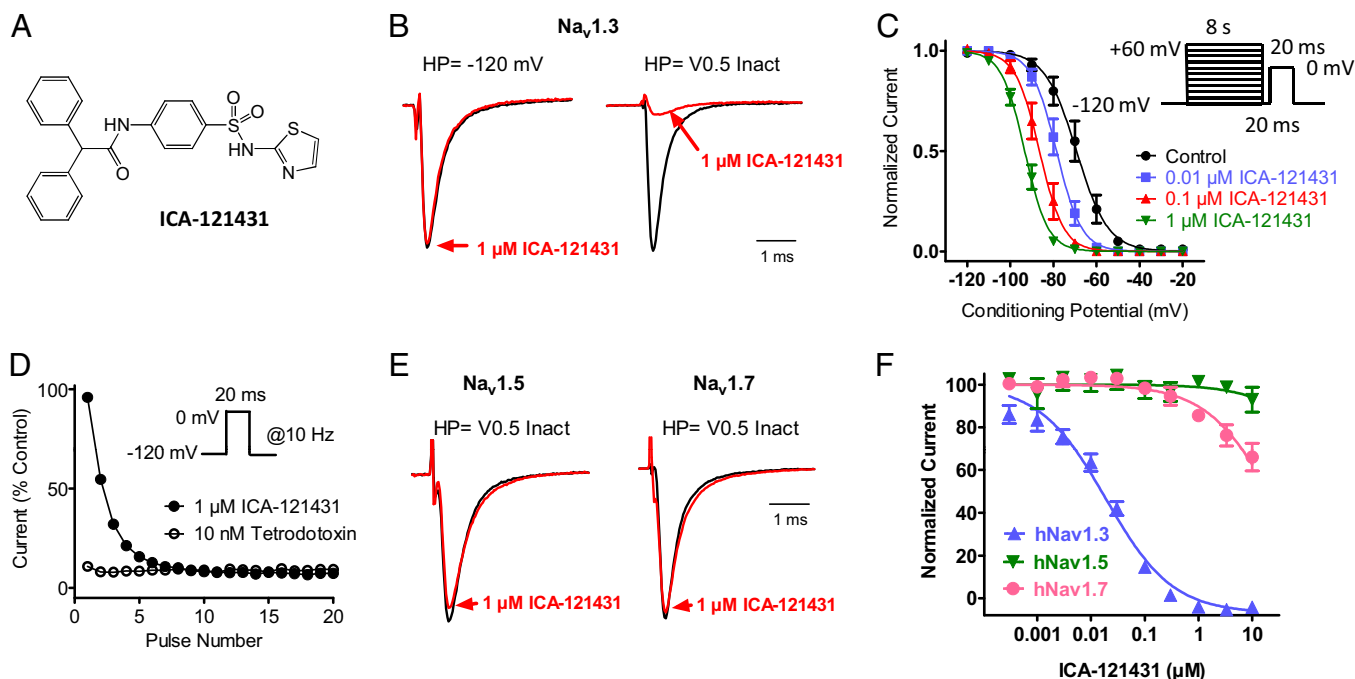


Fig. 1. Properties of Na_v channel inhibition by ICA-121431. (A) Structure of ICA-121431. (B) Current traces recorded on PatchXpress showing effect of $1 \mu\text{M}$ ICA-121431 on human $\text{Na}_v1.3$ current amplitude elicited by a 20-ms voltage step to 0 mV from -120 mV or after an 8-s conditioning voltage step (HP) to -60 mV to inactivate approximately half of the available channels. Current traces are normalized so that control traces have same relative amplitude. (C) Voltage dependence of human $\text{Na}_v1.3$ inactivation in the presence and absence of ICA-121431. Peak current amplitudes were measured during test pulses to 0 mV after an 8-s conditioning depolarization to the indicated potentials in the absence and presence of 0.01, 0.1, and $1 \mu\text{M}$ ICA-121431. Values from individual cells were normalized to the largest amplitude current after a prepulse to the most hyperpolarized conditioning potential (-120 mV). Normalized inactivation curves were fit with a Boltzmann equation, whereby the half inactivation voltage in the presence of ICA-121431 was -78 ± 2 mV ($0.01 \mu\text{M}$), -86 ± 2 mV ($0.1 \mu\text{M}$), and -93 ± 2 mV ($1 \mu\text{M}$) compared with -67 ± 2 mV in the absence of inhibitor. (D) Use dependent inhibition of human $\text{Na}_v1.3$ by $1 \mu\text{M}$ ICA-121431. Plot of current amplitude (normalized to control) during a train of 20-ms voltage steps from -120 mV to 0 mV given at 10 Hz in the presence of $1 \mu\text{M}$ ICA-121431 or 10 nM TTX. (E) PatchXpress recording showing effect of $1 \mu\text{M}$ ICA-121431 on human $\text{Na}_v1.5$ and $\text{Na}_v1.7$ currents elicited by a 20-ms voltage step to 0 mV after an 8-s condition voltage step to inactivate approximately half of the available channels. (F) Concentration dependence of human $\text{Na}_v1.3$, $\text{Na}_v1.5$, and $\text{Na}_v1.7$ inhibition by ICA-121431 [IC_{50} 18 ± 5 nM ($n = 6$) for $\text{Na}_v1.3$ and $>10 \mu\text{M}$ for $\text{Na}_v1.5$ ($n = 4$) and $\text{Na}_v1.7$ ($n = 6$), respectively]. Inhibition of sodium currents was recorded on IonWorks Quattro using a protocol comprising a 500-ms step from -120 mV to 0 mV to inactivate the channels, followed after a 100-ms recovery at -100 mV by a 20-ms test pulse to 0 mV to define inhibition.

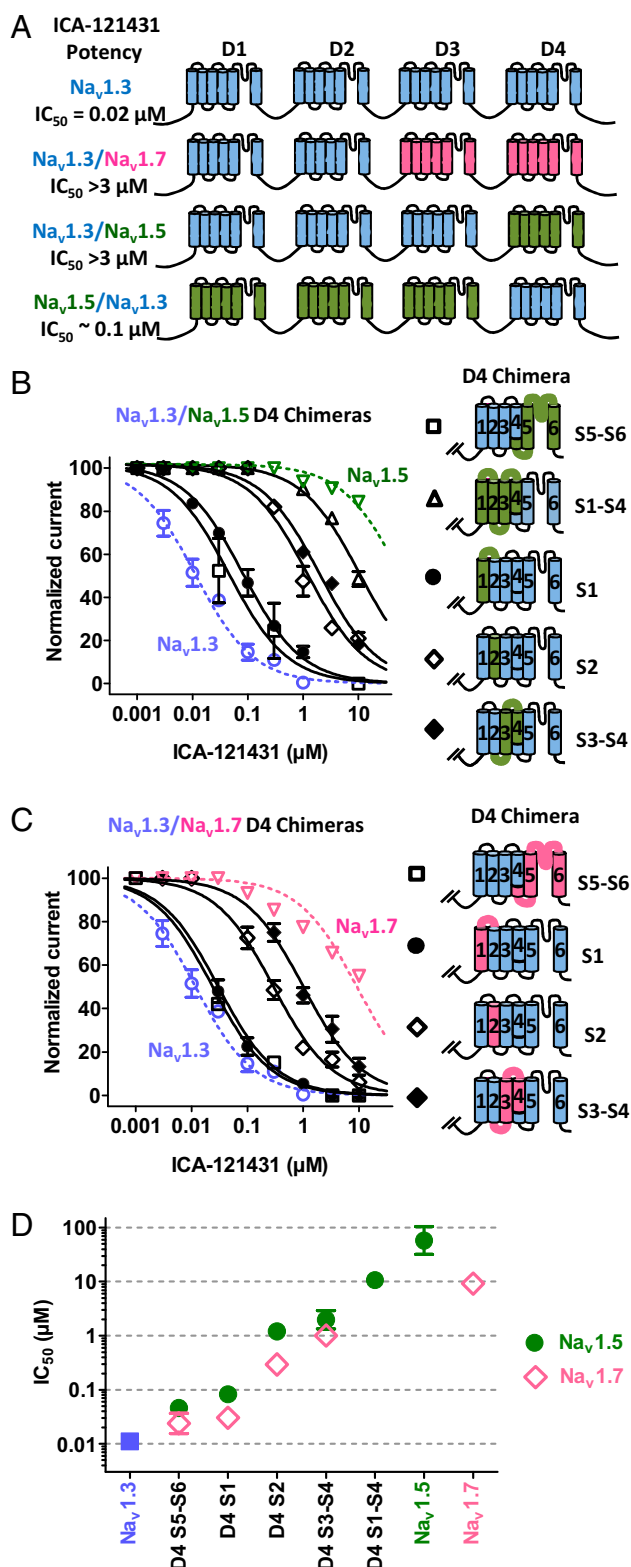


Fig. 2. (A) Defining interaction region on $Na_v1.3$ required for inhibition by ICA-121431. Relative potency of ICA-121431 inhibition of chimeric sodium channels comprising various domains of $Na_v1.3$ (blue) combined with domains from either $Na_v1.5$ (green) or $Na_v1.7$ (pink). Potent inhibition was only observed in chimeras containing a $Na_v1.3$ Domain 4. (B) Concentration dependence of ICA-121431 inhibition of $Na_v1.3$ sodium channel chimeras in which subregions of Domain 4 have been replaced with equivalent regions from $Na_v1.5$ are compared with inhibition of unmodified $Na_v1.3$ (blue) or $Na_v1.5$ (green). (C) Concentration dependence of ICA-121431 inhibition of

amino acid residues that may define selectivity for this channel over other related Na_v channels, including $Na_v1.7$ and $Na_v1.5$. Our initial attempts focused on establishing whether inhibition resulted from interaction with a specific domain of the sodium channel. Restriction sites were introduced into the nucleotide sequences between the Domain 1–4 repeats of $Na_v1.3$, $Na_v1.7$, and $Na_v1.5$ (details of sites in Fig. S2). Chimeras of $Na_v1.3$ domains combined with varying homologous domains of either $Na_v1.7$ or $Na_v1.5$ were constructed and expressed in HEK-293 cells and then evaluated for inhibition by ICA-121431 using the 8-s half inactivation pulse protocol on conventional patch clamp described previously. Fig. 2A shows that replacement of Domain 3 and 4 of $Na_v1.3$ with the equivalent domains from $Na_v1.7$ resulted in a chimeric channel (Domains 1–4 = 3,3,7,7) that exhibited very weak sensitivity to inhibition by ICA-121431 ($12\% \pm 4\%$ at $3 \mu M$, $n = 3$). This data suggested that the interaction site may lie somewhere within homologous Domains 3 and 4. Another chimera in which only Domain 4 of $Na_v1.3$ was replaced with the equivalent domain from $Na_v1.5$ (Domains 1–4 = 3,3,3,5) also lacked sensitivity to inhibition by ICA-121431 ($19\% \pm 4\%$ at $3 \mu M$, $n = 3$). These findings suggest that Domain 4 may contain an interaction site for ICA-121431 inhibition. Further support of this hypothesis was demonstrated when a chimera comprising Domains 1–3 of $Na_v1.5$ and Domain 4 of $Na_v1.3$ (Domains 1–4 = 5,5,5,3) exhibited relatively potent inhibition by ICA-121431 ($45\% \pm 2\%$ at $0.1 \mu M$ and $90\% \pm 3\%$ at $1 \mu M$, $n = 2$) (Fig. 2A), which is \sim fivefold less potent than $Na_v1.3$ but more than 500-fold more potent than inhibition of $Na_v1.5$. It further suggests that the entire ICA-121431 interaction site may be contained within Domain 4 of $Na_v1.3$.

It should be noted that the chimeras described above do exhibit significant differences in the voltage dependence of inactivation relative to unmodified $Na_v1.3$ (midpoints of potentials of -73 ± 1 mV for 3,3,7,7 chimera, -67 ± 1 mV for 3,3,3,5 chimera; -82 ± 2 mV for 5,5,5,3 chimera compared with -58 ± 1 mV for wild-type $Na_v1.3$). However, we believe that by using an 8-s conditioning pulse to the midpoint of inactivation protocol set appropriately for each of the chimeras being evaluated, we minimized the contribution of differences in voltage dependence of inactivation to apparent potency differences. Support for this comes from the finding that $1 \mu M$ amitriptyline [a nonselective Na_v channel inhibitor that interacts preferentially with inactivated channels (34)] produced relatively similar inhibition of the chimeras compared with unmodified $Na_v1.3$; 40% for 3,3,7,7 chimera, 60% for 3,3,3,5 chimera; 35% for 5,5,5,3 chimera compared with 51% for wild-type $Na_v1.3$ (less than threefold differences in estimated IC_{50} s).

ICA-121431 Interacts with the Voltage Sensor Region in Domain 4 on $Na_v1.3$.

The apparent importance of Domain 4 for inhibition of $Na_v1.3$ by ICA-121431 was further evaluated by constructing chimeras with homologous Domains 1–3 from $Na_v1.3$ and various subregions of Domain 4 containing the equivalent amino acid residue sequences from either $Na_v1.5$ (Fig. 2B) or $Na_v1.7$ (Fig. 2C) (details of splice sites in Fig. S3). Replacement of Domain 4 S5 and S6 transmembrane regions of $Na_v1.3$ with those from $Na_v1.5$ or $Na_v1.7$ (S5–S6) produced only small changes (two- to fivefold decrease) in ICA-121431 potency. In contrast, replacement of the

$Na_v1.3$ sodium channel chimeras in which subregions of Domain 4 have been replaced with equivalent regions from $Na_v1.7$ are compared with inhibition of unmodified $Na_v1.3$ (blue) or $Na_v1.7$ (pink). (D) IC_{50} s for ICA-121431 inhibition of various $Na_v1.3$ - $Na_v1.5$ or $Na_v1.3$ - $Na_v1.7$ Domain 4 chimeras compared with unmodified $Na_v1.3$, $Na_v1.5$, and $Na_v1.7$. Values are means \pm SEM ($n = 4$ –22). Inhibition of sodium currents in B, C, and D were recorded using conventional patch clamp and determined using an 8-s conditioning voltage step from -120 mV to a voltage producing half-maximal inactivation followed after a 20-ms recovery at -100 mV by a 20-ms test pulse to 0 mV.

Domain 4 voltage sensor region S1–S4 of $\text{Na}_v1.3$ with the same region from $\text{Na}_v1.5$ (S1–S4) resulted in a >500-fold loss potency for inhibition by ICA-121431 (IC_{50} $10 \pm 2 \mu\text{M}$, $n = 3$) (Fig. 2B–D), indicating that the main interaction site for ICA-121431 probably lies within the voltage sensor region.

To further delineate possible interaction sites within the Domain 4 S1–S4 voltage sensor region, three additional chimeras were constructed, in which either the S1, S2, or S3–S4 transmembrane segments or associated loops from Domain 4 of the $\text{Na}_v1.3$ were replaced with the equivalent amino acid sequences of $\text{Na}_v1.5$ or $\text{Na}_v1.7$ (Fig. 2B and C). Fig. 2D shows that whereas replacing S1 of $\text{Na}_v1.3$ with S1 from $\text{Na}_v1.5$ or $\text{Na}_v1.7$ produced a relatively small (three- to eightfold) reduction in inhibition potency, replacement of either S2 or S3–S4 with the $\text{Na}_v1.5$ or

$\text{Na}_v1.7$ sequence resulted in 20- to 100-fold loss in sensitivity to inhibition by ICA-121431 (IC_{50} s for different chimeras are summarized in Table S2).

Three Amino Residues in the Voltage Sensor Region Contribute to Selectivity of ICA-121431. To identify specific amino acid residues within the S2–S4 region of Domain 4 that contribute to ICA-121431 selective inhibition, we aligned human Na_v channel amino acid sequences of Domain 4 S1–S4 and then grouped by relative sensitivity to inhibition. As noted earlier, the two most sensitive channels were $\text{Na}_v1.3$ and $\text{Na}_v1.1$. $\text{Na}_v1.2$ exhibited an intermediate sensitivity (IC_{50} 240 nM), whereas $\text{Na}_v1.4$, $\text{Na}_v1.5$, $\text{Na}_v1.6$, $\text{Na}_v1.7$, and $\text{Na}_v1.8$ were relatively insensitive to inhibition (IC_{50} s >10 μM) (Fig. 3A, Fig. S1, and Table S1).

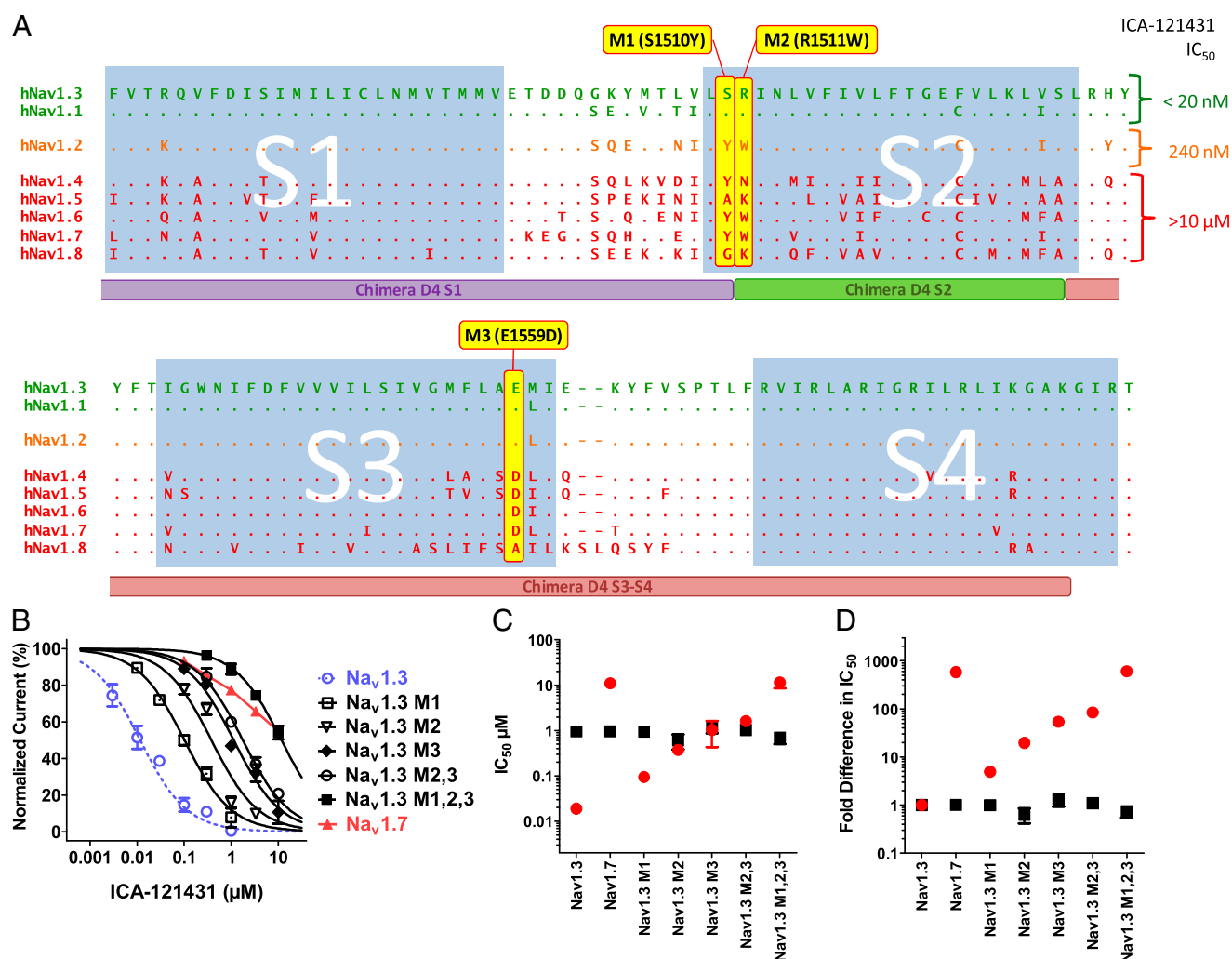


Fig. 3. Defining amino acid residues important for inhibition of $\text{Na}_v1.3$ by ICA-121431. (A) Comparison of amino acid sequence for S1–S4 voltage-sensor region of Domain 4 for different subtypes of human voltage dependent sodium channel. Residues that are different from $\text{Na}_v1.3$ are shown (i.e., dots represent residues that are identical to $\text{Na}_v1.3$). Sequence alignments for channels demonstrating high sensitivity to inhibition by ICA-121431 (IC_{50} <20 nM) are shown in green, intermediate sensitivity (IC_{50} ~300 nM) are shown in orange, and insensitive channels (IC_{50} >10 μM) are shown in red. Residues that were present in ICA-121431 sensitive channels but absent in insensitive sodium channels (highlighted in yellow) were mutated, substituting in equivalent residues from $\text{Na}_v1.7$ (termed M1, M2, and M3). The location of the chimera constructs D4 S1, D4 S2, and D4S3–S4 described in Fig. 2 are shown below the sequences for comparison. (B) Concentration dependence of ICA-121431 inhibition of human $\text{Na}_v1.3$ mutated to contain single or combinations of human $\text{Na}_v1.7$ residues at the three residue positions highlighted in A. Mutated $\text{Na}_v1.3$ channels are compared with unmodified $\text{Na}_v1.3$ (blue) and $\text{Na}_v1.7$ (red). (C) Comparison of IC_{50} for ICA-121431 (red circles) and amitriptyline (black squares) inhibition of $\text{Na}_v1.3$, $\text{Na}_v1.7$, and various combinations of $\text{Na}_v1.3$ M1 (S1510Y), M2 (R1511W), or M3 (E1559D) mutations. (D) Comparison of fold difference in IC_{50} for ICA-121431 (red circles) and amitriptyline (black squares) mediated inhibition of $\text{Na}_v1.7$ and various combinations of $\text{Na}_v1.3$ M1 (S1510Y), M2 (R1511W), or M3 (E1559D) mutations relative to wild-type human $\text{Na}_v1.3$. Data were generated using conventional patch clamp using an 8-s conditioning voltage step from -120 mV to a voltage producing half-maximal inactivation followed after a 20-ms recovery at -100 mV by a 20-ms test pulse to 0 mV.

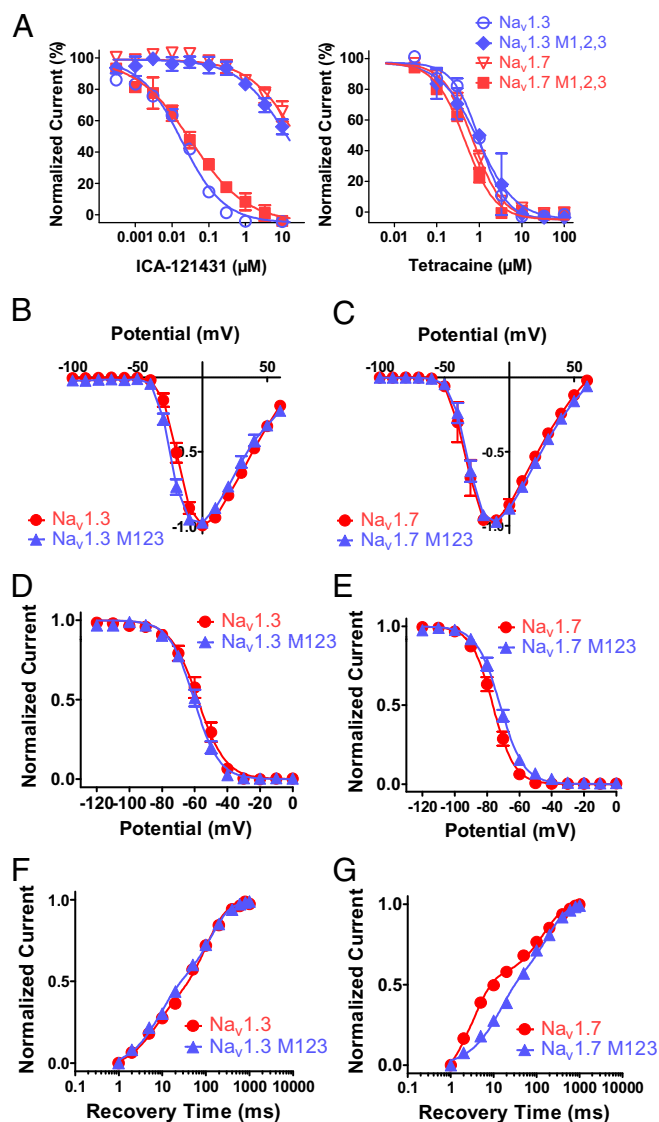


Fig. 4. Pharmacological and biophysical properties of Na_v1.3 and Na_v1.7 M123 triple mutant. (A) Comparison of inhibition by ICA-121431 (Left) or tetracaine (Right) after substituting the M1, M2, and M3 residues of Na_v1.3 with residues from Na_v1.7 (i.e., S1510Y/R1511W/E1559D) or vice versa in which the equivalent M1, M2, and M3 residues of Na_v1.7 are substituted with equivalent residues from Na_v1.3 (i.e., Y1537S/W1538R/D1586E). Inhibition was recorded using the IonWorks Quattro using the protocol described in Fig. 1F. Comparison of biophysical properties of human Na_v1.3 and the Na_v1.3 S1510Y/R1511W/E1559D triple mutant vs. human Na_v1.7 and the Na_v1.7 Y1537S/W1538R/D1586E triple mutant. (B and C) Current voltage relationships for wild-type and M123 mutant forms of Na_v1.3 and Na_v1.7. Peak current amplitudes were measured during 500-ms voltage steps to various membrane potentials from a holding potential of -120 mV. (D and E) Voltage dependence of inactivation for wild-type and M123 mutant forms of Na_v1.3 and Na_v1.7. Peak current amplitudes were measured during test pulses to -20 mV after 500-ms conditioning depolarizations to the indicated potentials. Individual normalized inactivation curves were fit with a Boltzmann equation, $1/(1 + \exp[(V_h - V)/k])$, where V_h is the half-inactivation voltage, and k is the slope. Values for V_h and k are shown in Table S3. (F and G) Time course of recovery from inactivation for wild-type and M123 mutant forms of Na_v1.3 and Na_v1.7. Peak current amplitudes were measured during test pulses to -20 mV after a variable time period after a 500-ms conditioning depolarization to 0 mV. Individual normalized recovery curves were fit with a two phase exponential association equation, $Y = \text{FractionFast} [1 - \exp(-t/\text{tauFast})] + \text{FractionSlow} [1 - \exp(-t/\text{tauSlow})]$, where Y is the fraction of total current amplitude at time, t , and comprises fraction of current recovering with fast kinetics, FractionFast at time constant, tauFast or recovering with

Focusing on the S2–S4 region of Domain 4, we looked for amino acid residues shared between Na_v1.3 and Na_v1.1 and not most other Na_v channels. Three residues were identified: consecutive serine and arginine residues at positions 1510 and 1511 and a glutamate at position 1559 in S3 of Na_v1.3 (Fig. 3A). S1510, R1511, and E1559 are predicted to be at the extracellular ends of the S2 and S3 transmembrane segments and were therefore initially considered to be promising candidates for potential ligand interaction. To examine their role, individually and together, these Na_v1.3 residues were replaced with the equivalent residues of the ICA-121431-insensitive Na_v1.7 channel. The effects of these mutations on inhibition by ICA-121431 are shown in Fig. 3B (also refer to Table S2). S1510Y (M1) resulted in a ninefold loss of potency of ICA-121431, whereas R1511W (M2) and E1559D (M3) produced 33-fold and 97-fold reductions in potency, respectively. The double mutation R1511W/E1559D (M2,3) produced a 152-fold loss of potency, whereas the triple mutation S1510Y/R1511W/E1559D (M1,2,3) resulted in a 600-fold loss of potency, exhibiting a lack of sensitivity to inhibition by ICA-121431 similar to Na_v1.7. These results suggest that all three identified residues on Na_v1.3 play a role in defining inhibition by ICA-121431. Although variations in the voltage dependence of inactivation for the various mutants were observed (Fig. S2), for the most part they were <7 mV and there was no obvious correlation with the widely varying potencies seen with ICA-121431. Moreover, all of the individual (M1, M2, M3) and multiple mutants (M2,3 and M1,2,3) of Na_v1.3 exhibited relatively constant sensitivities to inhibition by amitriptyline ($IC_{50} \sim 1 \mu\text{M}$) (Fig. 3C and D), which as mentioned earlier would be expected to exhibit similar sensitivity to differences in the voltage dependence of inactivation as ICA-121431.

An obvious next question is whether the S1510/R1511/E1559 residues are sufficient to account for the selectivity of ICA-121431 for Na_v1.3 over Na_v1.7. To address this question, a triple mutation of Na_v1.7 was made in which residues corresponding to M1, M2, and M3 were replaced by the equivalent Na_v1.3 residues (Y1537S/W1538R/D1586E; Na_v1.7 M1,2,3). Fig. 4A, Left compares ICA-121431 inhibition of Na_v1.7 M1,2,3 with Na_v1.3 M1,2,3, wild-type Na_v1.3, and Na_v1.7. Replacement of the three residues on Na_v1.7 with those from Na_v1.3 resulted in an 860-fold increase in potency for inhibition by ICA-121431; Na_v1.7 M1,2,3 exhibited an IC_{50} of 33 nM, which is within twofold of the IC_{50} of 18 nM for unmodified Na_v1.3. Furthermore, in contrast to the dramatic effects of Na_v1.7 M1,2,3 and Na_v1.3 M1,2,3 on ICA-121431 inhibition, these mutations had little or no effect on inhibition by the local anesthetic tetracaine (Fig. 4A, Right). Moreover, the M1,2,3 mutant forms of either Na_v1.3 or Na_v1.7 were associated with only minimal changes in biophysical properties, such as voltage dependence of activation (Fig. 4B and C), inactivation (Fig. 4D and E), and rate of recovery from inactivation (Fig. 4F and G) (Table S3 lists biophysical parameters). These nominal biophysical differences are unlikely to account for the profound changes in pharmacological sensitivity seen in the mutated channels. Therefore, taken together, the evidence suggests that the S1510/R1511/E1559 residues in the Domain 4 voltage sensor region of Na_v1.3 contribute to the potent and selective inhibition of Na_v1.3 (and Na_v1.1) by ICA-121431 by affecting the physical interaction of the molecule.

The Same Three Amino Residues Can Contribute to Human Na_v1.7 Inhibitor Selectivity.

The selectivity profile of ICA-121431, along with amino acid sequence diversity among Na_v family members

slow kinetics, FractionSlow at time constant, tauSlow. Values for time constants, tauFast, and tauSlow and fraction of current recovering with fast kinetics FractionFast are shown in Table S3. Data were generated using the PatchXpress automated electrophysiology platform.

around the proposed interaction site (Fig. 3A), raises the question of whether this region of Na_v channels provides opportunities for finding inhibitors with selectivity for other Na_v channel subtypes. This question was addressed with another aryl sulphonamido-thiazole-containing molecule, PF-04856264 [3-cyano-4-(2-(1-methyl-1H-pyrazol-5-yl) phenoxy)-*N*-(thiazol-2-yl) benzenesulfonamide] (Fig. 5A), which was identified during a screen for $\text{Na}_v1.7$ inhibitors. PF-04856264 was observed to interact preferentially with the inactivated state of $\text{Na}_v1.7$. Fig. 5B shows that $\text{Na}_v1.7$ currents elicited by 20-ms depolarizing voltage steps from -120 mV were insensitive to inhibition by $1 \mu\text{M}$ PF-04856264, whereas the same concentration produced $91\% \pm 4\%$ inhibition when a test pulse was preceded by an 8-s conditioning voltage step to inactivate approximately half of the channels. Interestingly, using this latter protocol, human $\text{Na}_v1.3$ and $\text{Na}_v1.5$ exhibited little or no sensitivity to inhibition by $1 \mu\text{M}$ PF-04856264 (Fig. 5C). The subtype selectivity exhibited by PF-04856264 is further illustrated in the concentration response curves shown in Fig. 5D (generated using the same protocol used for ICA-121431 in Fig. 1D). The fitted IC_{50} for inhibition of human $\text{Na}_v1.7$ was 28 ± 5 nM ($n = 8$), whereas little or no inhibition of human $\text{Na}_v1.3$ or $\text{Na}_v1.5$ currents were observed at concentrations up to $10 \mu\text{M}$.

Given the structural similarity (i.e., aryl sulphonamido-thiazole moiety) between PF-04856264 and ICA-121431, we evaluated the importance of the Domain 4 voltage sensor M1,2,3 residues of $\text{Na}_v1.7$ for PF-04856264 inhibitor activity. Fig. 5E shows that when the M1,2,3 equivalent residues on $\text{Na}_v1.7$ were substituted with residues found in $\text{Na}_v1.3$ (i.e., Y1537S/W1538R/D1586E), inhibition by PF-04856264 was essentially abolished ($\text{IC}_{50} > 10 \mu\text{M}$). The specificity of this modulatory effect is highlighted by the finding that inhibition by other established sodium channel blocking agents, tetracaine and TTX, which reportedly bind within or over the pore, was not changed by the Y1537S/W1538R/D1586E substitution (Fig. 5F and G). Fur-

thermore, Fig. 5E and F provide supporting evidence that PF-04856264 and local anesthetic-like inhibitors interact with distinct binding sites, because mutation of two residues (F1737A/Y1744A) in S6 of Domain 4 of $\text{Na}_v1.7$, which are reported to be involved in local anesthetic and antiepileptic drug binding to Na_v channels (19, 20), resulted in a >100 -fold loss of potency for inhibition by tetracaine ($\text{IC}_{50} > 100 \mu\text{M}$ compared with $0.9 \mu\text{M}$ for wild-type $\text{Na}_v1.7$) but only a nominal change in the potency of PF-04856264 ($\text{IC}_{50} = 12$ nM compared with 28 nM for wild-type $\text{Na}_v1.7$).

To further evaluate whether the M123 Y1537/W1538/D1586 amino acid motif was sufficient to account for the $\text{Na}_v1.7$ vs. $\text{Na}_v1.3$ selectivity observed with PF-04856264, a construct was generated in which the equivalent residues of human $\text{Na}_v1.3$ were replaced with the $\text{Na}_v1.7$ M123 residues (S1510Y/R1511W/E1559D). The potency for inhibition of $\text{Na}_v1.3$ M123 (S1510Y/R1511W/E1559D) by PF-04856264 was found to be $7 \mu\text{M}$. Although this IC_{50} is measurably lower than for $\text{Na}_v1.7$ M123 (Y1537S/W1538R/D1586E), it is 250-fold greater than the IC_{50} for wild-type $\text{Na}_v1.7$. These findings suggest that although the M123 residues are important for PF-04856264 inhibition of $\text{Na}_v1.7$, they are not sufficient to account for all of the subtype selectivity observed with this particular inhibitor, indicating that additional residues in this region may play a role in determining subtype selective interactions.

Species Dependent Inhibition by ICA-121431 and PF-04856264 Is Determined by Amino Acid Sequence Differences in Domain 4 Voltage Sensor Region.

Although we have shown that ICA-121431 and PF-04856264 exhibit selectivity for human $\text{Na}_v1.3$ or human $\text{Na}_v1.7$, this profile was not observed with all mammalian species evaluated. For example, whereas cynomolgus monkey and dog $\text{Na}_v1.7$ lacked sensitivity to inhibition by ICA-121431 ($\text{IC}_{50s} > 5,000$ nM) similar to human $\text{Na}_v1.7$, we found that rat

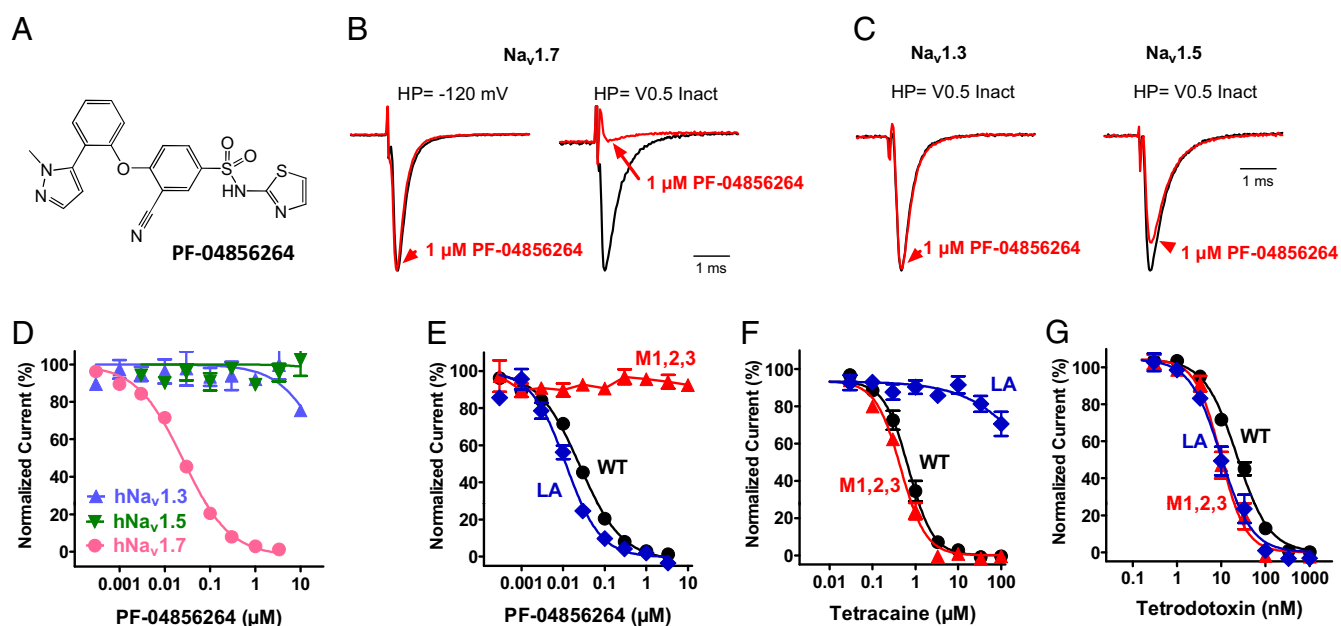


Fig. 5. Selective $\text{Na}_v1.7$ inhibitor also interacts with Domain 4 voltage sensor. (A) Structure of PF-04856264. (B) Current traces recorded on PatchXpress showing effect of $1 \mu\text{M}$ PF-04856264 on human $\text{Na}_v1.7$ current amplitude elicited by a 20-ms voltage step to 0 mV from -120 mV or after an 8-s condition voltage step to -75 mV to inactivate approximately half of the available channels. Current traces are normalized so that control traces have same relative amplitude. (C) PatchXpress recording showing effect of $1 \mu\text{M}$ PF-04856264 on human $\text{Na}_v1.3$ and $\text{Na}_v1.5$ currents elicited by a 20-ms voltage step to 0 mV after an 8-s condition voltage step to inactivate approximately half of the available channels. (D) Concentration dependence of inhibition of human $\text{Na}_v1.3$, $\text{Na}_v1.5$, and $\text{Na}_v1.7$ currents by PF-04856264 (IC_{50} is 28 ± 5 nM for $\text{Na}_v1.7$ and $>10 \mu\text{M}$ for $\text{Na}_v1.3$ and $\text{Na}_v1.5$). (E) PF-04856264 mediated inhibition of unmodified (WT) $\text{Na}_v1.7$, $\text{Na}_v1.7$ M1,2,3 (Y1537S/W1538R/D1586E), or the local anesthetic binding site mutant $\text{Na}_v1.7$ (F1737A/Y1744A) (LA) compared with inhibition by the local anesthetic tetracaine (F) or TTX (G). IC_{50s} are provided in the text. Data for D–G were generated on the IonWorks Quattro using the protocol described in Fig. 1F.

Na_v1.7 is potently inhibited by ICA-121431 with an IC₅₀ of 19 nM, which is more comparable to its inhibition of human Na_v1.3 (i.e., >1,000-fold more potent than human Na_v1.7) (Fig. 6A). However, mouse Na_v1.7 gave a more human-like profile, with an IC₅₀ for inhibition by ICA-121431 of 8,700 nM. Intriguingly, an opposite differential rodent sensitivity to inhibition was observed with the human Na_v1.7-selective inhibitor PF-04856264 (Fig. 6B). Whereas the IC₅₀s for PF-04856264 inhibition of cynomolgus monkey (19 nM) or dog Na_v1.7 (42 nM) were comparable to human Na_v1.7, rat Na_v1.7 was considerably less sensitive, exhibiting an IC₅₀ of 4,200 nM. Again, in contrast to rat, mouse Na_v1.7 exhibited a higher sensitivity to inhibition by PF-04856264 (IC₅₀ 131 nM).

The amino acid sequence alignments of the Domain 4 S1–S4 transmembrane segments from Na_v1.7 for different species shown in Fig. 6C provide a possible explanation for the variation in species sensitivities to inhibition by ICA-121431 or PF-04856264. Although there is a high degree of sequence homology across species in this region, there are notable variations including those in the M1, M2, or M3 residues (i.e., human Na_v1.7-Y1537/W1538/D1586), which have been shown in previous sections to be important for defining human Na_v1.3 and Na_v1.7 selectivity. Specifically, species exhibiting the most human-like Na_v1.7 inhibition profile (i.e., cynomolgus monkey, dog, and mouse Na_v1.7) also exhibited the highest sequence homology over these three residues. In contrast, rat Na_v1.7 differs at both the M1 and M3 residues.

Discussion

In the present study we characterize a unique class of nanomolar potent small molecule inhibitors of Na_v channels that interact with and stabilize inactivated states of the channel. Furthermore, structurally related compounds within this class exhibit subtype selective inhibition of Na_v channels, including human Na_v1.3 and Na_v1.7. For example, ICA-121431 exhibited a spectrum of inhibitory activity for Na_v human channel subtypes; equipotent inhibition of Na_v1.3 and Na_v1.1, less potent inhibition of Na_v1.2, and much weaker inhibition of Na_v1.7, Na_v1.6, Na_v1.4, and the TTX-resistant human Na_v1.5 and Na_v1.8 channels (IC₅₀s >10 μM). We exploited the subtype selectivity of ICA-121431 to investigate possible Na_v interaction sites by constructing Na_v1.3/Na_v1.5 or Na_v1.7 chimeras. Functional evaluation of these chimeras has provided evidence that the likely site of interaction for this class of inhibitor is at extracellular ends of the S2 and S3 transmembrane segments of Domain 4. By comparing the amino acid sequences of ICA-121431 sensitive vs. insensitive Na_v channel subtypes over this region of the voltage sensor, we have identified three unique

residues found only in channels sensitive to inhibition by ICA-121431 [S1510 (M1), R1511 (M2), and E1559 (M3) of Na_v1.3]. Their replacement with equivalent residues from the ICA-121431-insensitive Na_v1.7 channel reduced potency for Na_v1.3 inhibition by >500-fold. Further compelling evidence that the M1,2,3 residues are primary contributors to selective inhibition of Na_v1.3 by ICA-121431 came from substituting the three M1,2,3 residues in human Na_v1.7 with the Na_v1.3 equivalent residues (Y1537S/W1538R/D1586E), which resulted in a striking gain in sensitivity to inhibition, comparable to unmodified Na_v1.3. Although each of the M1, M2, or M3 residues contribute to inhibition, modification of the M2 and M3 residues alone and in combination had the largest impact on potency of ICA-121431. The M1,2,3 residues also seem to contribute to the inhibition of Na_v1.7 by PF-04856264 given the substantial reduction of inhibition with replacement of the equivalent residues from human Na_v1.3. Furthermore, the finding that both Na_v1.3 and Na_v1.7 selective inhibitors interact with similar but not entirely equivalent regions of the Domain 4 S2/S3 transmembrane segment indicates that additional interactions exist, possibly including residues that are conserved across Na_v channel subtypes in this region of the voltage sensor domain. An improved understanding of the functional importance of residues in and around the identified M1,2,3 residues may enable a fuller appreciation of the potential diversity of Na_v subtype selective interactions that may be determined by this site.

As described, the dramatic changes in potency of ICA-121431 and PF-04856264 induced by modifications of the M1, M2, or M3 residues are unlikely to result from global structural rearrangements, because inhibition of individual or combined M1,2,3 Na_v1.3 mutants (Na_v1.3-S1510Y/R1511W/E1559D) or Na_v1.7 M123 (Na_v1.7-Y1537S/W1538R/D1586E) by amitriptyline, tetracaine, or TTX was comparable to wild-type channels. Furthermore, the absence of effect on local anesthetic-mediated inhibition suggests that Na_v channel inactivation gating is not significantly affected by the M1,2,3 residue modifications. Indeed, an evaluation of the activation and inactivation gating properties of Na_v1.3-S1510Y/R1511W/E1559D or Na_v1.7-Y1537S/W1538R/D1586E are insufficient to account for the pharmacological changes observed.

Interestingly, observed species differences in sensitivity to inhibition by ICA-121431 or PF-04856264 can also be explained by differences in the M1,2,3 residue motif. The variability in species sensitivity to sodium channel inhibitors like the ones described in this study highlight the importance of gathering such information before evaluating compound efficacy and/or toxicity in animal tissues or in vivo models.

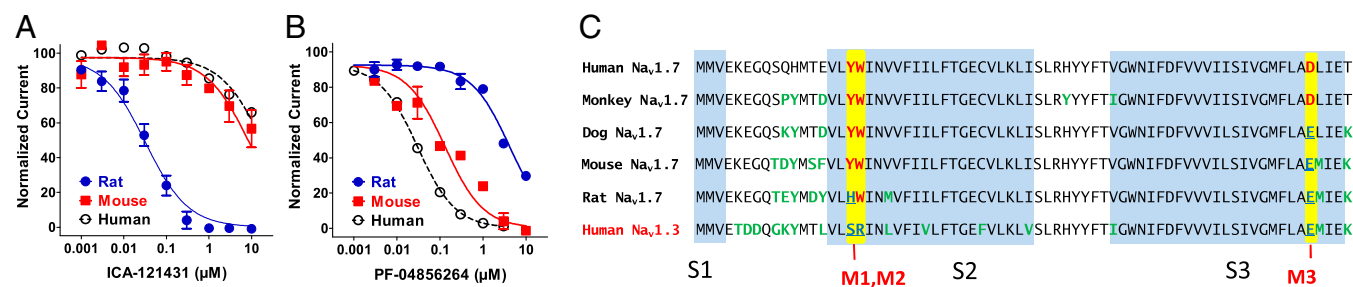


Fig. 6. Species orthologs of Na_v1.7 exhibit different sensitivities to inhibition by ICA-121431 and PF-04856264. (A) Concentration dependent inhibition of rat Na_v1.7 (blue squares), mouse Na_v1.7 (red squares), and human Na_v1.7 (black open circles) by ICA-121431. The fitted IC₅₀s are 37 nM (rat), 8,800 nM (mouse), and >10,000 nM (human). (B) Concentration dependent inhibition of rat Na_v1.7 (blue squares), mouse Na_v1.7 (red circles), and human Na_v1.7 (black open circles) by PF-04856264. The fitted IC₅₀s are 4200 nM (rat), 131 nM (mouse), and 30 nM (human). (C) Amino acid sequence alignment of various species orthologs of Na_v1.7 homologous Domain 4 transmembrane segments S1–S3 (light blue). Residues highlighted in yellow are the M1, M2, and M3 described in the text, which contribute to defining hNa_v1.3 vs. hNa_v1.7 selectivity by ICA-121431 and PF-04856264. Differences from human Na_v1.7 sequence within M1,2,3 are colored blue and underlined. Other sequence differences across species are colored green.

The present study provides compelling evidence that the unique subtype selective Na_v channel inhibitors ICA-121431 and PF-04856264 interact with amino acid residues on an extracellular facing region of the homologous Domain 4 voltage sensor of Na_v1.3 or Na_v1.7, which is distinct from previously described interaction sites for TTX (12, 13) or local anesthetic-like (11, 20–22) Na_v channel inhibitors (Figs. S4 and S5 show homology models illustrating relative locations of interaction sites). However, this small molecule interaction region on Domain 4 does overlap with the interaction sites for a number of polypeptide toxin modulators of sodium channel function (6, 14, 15, 18). For example, at least one residue, E1559 on Na_v1.3 or D1586 on Na_v1.7 (M3 residue), which contributes to the interaction of both ICA-121431 and PF-04856264, is also important for interaction of site 3 scorpion venom and anemone toxins that slow Na_v channel inactivation (14, 15, 18, 35). The contribution of the M1 and M2 residues to peptide toxin binding is less well defined, although it has been reported that substitution of the tyrosine with alanine at position 1564 of Na_v1.2 (equivalent to M1 residue position described in this study) has no effect on Lqh2 scorpion toxin-induced slowing of inactivation (18).

Inhibition of Na_v channel function via interaction with the voltage sensor region has previously been reported for spider (e.g., Protx II, HWTX-IV) and marine snail (MuO conotoxins) peptide toxins (16, 36–38), although much of the published data suggest that they primarily interact with the voltage sensor of homologous Domain 2 (16, 17, 38–40). Several recent reports have also described possible interactions of Protx II with Domain 1, 3, and 4 voltage sensors (38–40). Interestingly, a residue equivalent to the Domain 4 M3 site on Na_v1.3 and Na_v1.7 has been reported to contribute to the interaction of Protx II, although this site may be more involved in a slowing of inactivation seen with the toxin rather than the more widely described inhibitory action (38). The mechanistic implications of preferential interactions with specific homologous domain voltage sensor regions by peptide vs. small molecule Na_v channel inhibitors remain to be fully explored. However, these differences may underlie the contrasting ability of peptide toxins like Protx II to inhibit Na_v channels by shifting the apparent voltage dependence of activation to depolarized potentials vs. apparent stabilization of one or more inactivated conformations by the small molecule inhibitors described in this study.

In conclusion, the present study highlights unique possibilities for identifying additional subtype selective small molecule sodium channel modulators by targeting allosteric interaction sites away from the pore region like those that contribute to voltage sensing and/or conformational changes associated with channel gating. Although the present studies have identified several residues on the Domain 4 voltage sensor region that are important for interaction and selectivity, further investigation is needed to elucidate the full extent of the interaction, perhaps by evaluating other residues reported to participate in peptide modulation of voltage sensor domains. Future studies will also be directed toward better understanding how pharmacological interactions with the voltage sensor in Domain 4 results in inhibition of conduction. Given the proposed involvement of Na_v channels in pain, cardiovascular, and central nervous system disorders (9, 41–45), further exploration of subtype selective Na_v channel inhibitors targeting this unique interaction site may provide opportunities to develop future voltage dependent Na channel directed therapeutics (27).

Methods

Reagents. ICA-121431 and PF-04856264 were synthesized by the medicinal chemistry group at IcaGen Inc. Tetracaine, amitriptyline, and TTX were obtained from Sigma Aldrich.

Generation of Chimeras and Mutants. Chimeric channels comprising human Na_v1.3, Na_v1.5, and Na_v1.7 domains and subdomains were assembled using

unique restriction enzyme sites introduced by site-directed mutagenesis in the respective channel coding regions (QuikChange II Site-Directed Mutagenesis and QuikChange Multi Site-Directed Mutagenesis kits; Stratagene). Not I and Sal I restriction sites allowed transfer of full-length cDNA constructs into either pcDNA3.1 (Invitrogen) or pLNCX2 (BD Bioscience Clontech) mammalian expression vectors. All intermediate and final constructs were verified by sequencing and are based on nucleotide numbering from National Center for Biotechnology Information GenBank sequences NM_006922 for hNa_v1.3 and NM_198056 for hNa_v1.5 and NM_002977 for hNa_v1.7. Final constructs were either transiently expressed (domain swap chimeras) or stably expressed (sub-Domain 4 chimeras and all point mutations) in HEK-293 cells. Transient transfections were achieved using Fugene 6 (Roche Applied Science) according to the vendor's protocol. Functional currents were recorded 48 h after transfections. Stable clonal cell lines were selected with G-418 (800 μg/mL) and prioritized by functional sodium current amplitude using conventional patch clamp or the IonWorks high-throughput electrophysiology platform. Controls for the wild-type human Na_v1.3, Na_v1.5, and Na_v1.7 were stably expressed in HEK-293 cells using the same procedures described above.

Electrophysiology. Functional characterization of voltage-gated sodium currents was accomplished using either conventional whole cell patch clamp or PatchXpress or Ionworks Quattro high-throughput electrophysiology platforms (Molecular Devices).

Conventional patch clamp. Coverslips containing HEK-293 cells expressing unmodified and mutated Na_v channels were placed in a recording chamber on the stage of an inverted microscope and perfused (~1 mL/min) with an extracellular solution containing 138 mM NaCl, 2 mM CaCl₂, 5.4 mM KCl, 1 mM MgCl₂, 10 mM glucose, and 10 mM Hepes (pH 7.4), with NaOH. Recording patch pipettes were filled with an intracellular solution containing 135 mM CsF, 5 mM NaCl, 2 mM MgCl₂, 10 mM EGTA, and 10 mM Hepes (pH 7.3) with NaOH and had a resistance of 1–2 MΩ. All recordings were made at room temperature (22–24 °C) using AXOPATCH 200B amplifiers and PCLAMP software (Molecular Devices). Na_v currents were measured using the whole-cell configuration of the patch clamp technique. All compounds were dissolved in DMSO to make 10-mM stock solutions, which were then diluted into extracellular solution to attain the final concentrations desired. The final concentration of DMSO (<0.3%) was found to have no significant effect on sodium currents. Test compound effects were evaluated using a protocol in which cells depolarized from a holding potential of –120 mV (or –140 mV for Na_v1.5) to a membrane potential that inactivated half of the available channels for 8 s (determined empirically for each channel type) followed after a 20-ms recovery at –120 mV by a test pulse to 0 mV to assess magnitude of inhibition. Concentration response data were analyzed using nonlinear least-squares fit of the Logistic Equation (GraphPad Prism 5) to provide IC₅₀ determinations.

PatchXpress automated electrophysiological platform. All assay buffers and solutions were identical to those used in conventional whole-cell voltage clamp experiments described above. Na_v channel-expressing cells were grown as above to 50–80% confluency and harvested by trypsinization. Trypsinized cells were washed and resuspended in extracellular buffer at a concentration of 1 × 10⁶ cells/mL. The onboard liquid handling facility of the PatchXpress was used for dispensing cells and application of test compounds. Test compound effects were evaluated and analyzed using the same protocols used for conventional patch clamp.

Ionworks Quattro automated electrophysiological platform. Intracellular and extracellular solutions were as described above with the following changes: 100 μg/mL amphotericin was added to the intracellular solution to perforate the membrane and allow electrical access to the cells. Na_v channel-expressing cells were grown and harvested as for PatchXpress, and cells were resuspended in extracellular solution at a concentration of 3–4 × 10⁶ cells/mL. The onboard liquid handling of the Ionworks Quattro was used for dispensing cells and application of test compounds. Test compound effects were evaluated using a voltage protocol in which a 500-ms voltage step to 0 mV from –120 mV was applied to fully inactivate available sodium channels, followed after a 50 ms to 100 s hyperpolarized recovery period at –120 mV to allow partial recovery from inactivation, by a test voltage step to 0 mV to assess magnitude of inhibition. This protocol facilitates comparison of channel subtypes independent of their differences in midpoint potentials for voltage dependence of inactivation.

ACKNOWLEDGMENTS. We thank Andrew Maynard, Aaron Gerlach, Sally Stoehr, Anrou Zuo, Theresa Mersch, Louise Heath, and Eva Prazak for additional experimental and cell reagent provision support.

1. Bezanilla F (2006) The action potential: From voltage-gated conductances to molecular structures. *Biol Res* 39(3):425–435.
2. Hodgkin AL, Huxley AF (1952) A quantitative description of membrane current and its application to conduction and excitation in nerve. *J Physiol* 117(4):500–544.
3. Catterall WA (2012) Voltage-gated sodium channels at 60: Structure, function and pathophysiology. *J Physiol* 590(Pt 11):2577–2589.
4. Marban E, Yamagishi T, Tomaselli GF (1998) Structure and function of voltage-gated sodium channels. *J Physiol* 508(Pt 3):647–657.
5. Payandeh J, Scheuer T, Zheng N, Catterall WA (2011) The crystal structure of a voltage-gated sodium channel. *Nature* 475(7356):353–358.
6. Billen B, Bosmans F, Tytgat J (2008) Animal peptides targeting voltage-activated sodium channels. *Curr Pharm Des* 14(24):2492–2502.
7. Llewellyn LE (2009) Sodium channel inhibiting marine toxins. *Prog Mol Subcell Biol* 46:67–97.
8. Catterall WA, et al. (2007) Voltage-gated ion channels and gating modifier toxins. *Toxicon* 49(2):124–141.
9. Wood JN, Boorman J (2005) Voltage-gated sodium channel blockers; target validation and therapeutic potential. *Curr Top Med Chem* 5(6):529–537.
10. Yanagitate F, Strichartz GR (2007) Local anesthetics. *Handb Exp Pharmacol* (177): 95–127.
11. Fozzard HA, Sheets MF, Hanck DA (2011) The sodium channel as a target for local anesthetic drugs. *Front Pharmacol* 2:68.
12. Fozzard HA, Lipkind GM (2010) The tetrodotoxin binding site is within the outer vestibule of the sodium channel. *Mar Drugs* 8(2):219–234.
13. Noda M, Suzuki H, Numa S, Stühmer W (1989) A single point mutation confers tetrodotoxin and saxitoxin insensitivity on the sodium channel II. *FEBS Lett* 259(1): 213–216.
14. Leipold E, Lu S, Gordon D, Hansel A, Heinemann SH (2004) Combinatorial interaction of scorpion toxins Lqh-2, Lqh-3, and LqhalphaIT with sodium channel receptor sites-3. *Mol Pharmacol* 65(3):685–691.
15. Rogers JC, Qu Y, Tanada TN, Scheuer T, Catterall WA (1996) Molecular determinants of high affinity binding of alpha-scorpion toxin and sea anemone toxin in the S3-S4 extracellular loop in domain IV of the Na⁺ channel alpha subunit. *J Biol Chem* 271(27): 15950–15962.
16. Schmalhofer WA, et al. (2008) ProTx-II, a selective inhibitor of Nav1.7 sodium channels, blocks action potential propagation in nociceptors. *Mol Pharmacol* 74(5): 1476–1484.
17. Sokolov S, Kraus RL, Scheuer T, Catterall WA (2008) Inhibition of sodium channel gating by trapping the domain II voltage sensor with protoxin II. *Mol Pharmacol* 73(3):1020–1028.
18. Wang J, et al. (2011) Mapping the receptor site for alpha-scorpion toxins on a Na⁺ channel voltage sensor. *Proc Natl Acad Sci USA* 108(37):15426–15431.
19. Liu G, et al. (2003) Differential interactions of lamotrigine and related drugs with transmembrane segment IVS6 of voltage-gated sodium channels. *Neuropharmacology* 44(3):413–422.
20. Panigel J, Cook SP (2011) A point mutation at F1737 of the human Nav1.7 sodium channel decreases inhibition by local anesthetics. *J Neurogenet* 25(4):134–139.
21. Ragsdale DS, McPhee JC, Scheuer T, Catterall WA (1994) Molecular determinants of state-dependent block of Na⁺ channels by local anesthetics. *Science* 265(5179): 1724–1728.
22. Ragsdale DS, McPhee JC, Scheuer T, Catterall WA (1996) Common molecular determinants of local anesthetic, antiarrhythmic, and anticonvulsant block of voltage-gated Na⁺ channels. *Proc Natl Acad Sci USA* 93(17):9270–9275.
23. England S, de Groot MJ (2009) Subtype-selective targeting of voltage-gated sodium channels. *Br J Pharmacol* 158(6):1413–1425.
24. Bolognesi R, Tsialtas D, Vasini P, Conti M, Manca C (1997) Abnormal ventricular repolarization mimicking myocardial infarction after heterocyclic antidepressant overdose. *Am J Cardiol* 79(2):242–245.
25. Wolfe JW, Butterworth JF (2011) Local anesthetic systemic toxicity: Update on mechanisms and treatment. *Curr Opin Anaesthesiol* 24(5):561–566.
26. Catterall WA (2010) Ion channel voltage sensors: Structure, function, and pathophysiology. *Neuron* 67(6):915–928.
27. England S, Rawson D (2010) Isoform-selective voltage-gated Na(+) channel modulators as next-generation analgesics. *Future Med Chem* 2(5):775–790.
28. Mantegazza M, Curia G, Biagini G, Ragsdale DS, Avoli M (2010) Voltage-gated sodium channels as therapeutic targets in epilepsy and other neurological disorders. *Lancet Neurol* 9(4):413–424.
29. Tarnawa I, Bölskei H, Kocsis P (2007) Blockers of voltage-gated sodium channels for the treatment of central nervous system diseases. *Recent Patents CNS Drug Discov* 2(1):57–78.
30. Clare JJ (2010) Targeting voltage-gated sodium channels for pain therapy. *Expert Opin Investig Drugs* 19(1):45–62.
31. Dib-Hajj SD, et al. (2009) Voltage-gated sodium channels in pain states: Role in pathophysiology and targets for treatment. *Brain Res Brain Res Rev* 60(1):65–83.
32. Krafft DS, Bannan AW (2008) Sodium channels and nociception: Recent concepts and therapeutic opportunities. *Curr Opin Pharmacol* 8(1):50–56.
33. Ragsdale DS, Scheuer T, Catterall WA (1991) Frequency and voltage-dependent inhibition of type IIA Na⁺ channels, expressed in a mammalian cell line, by local anesthetic, antiarrhythmic, and anticonvulsant drugs. *Mol Pharmacol* 40(5):756–765.
34. Wang GK, Russell C, Wang SY (2004) State-dependent block of voltage-gated Na⁺ channels by amitriptyline via the local anesthetic receptor and its implication for neuropathic pain. *Pain* 110(1–2):166–174.
35. Gurevitz M (2012) Mapping of scorpion toxin receptor sites at voltage-gated sodium channels. *Toxicon* 60(4):502–511.
36. Bosmans F, Swartz KJ (2010) Targeting voltage sensors in sodium channels with spider toxins. *Trends Pharmacol Sci* 31(4):175–182.
37. Knapp O, McArthur JR, Adams DJ (2012) Conotoxins targeting neuronal voltage-gated sodium channel subtypes: potential analgesics? *Toxins (Basel)* 4(11):1236–1260.
38. Xiao Y, Blumenthal K, Jackson JO, 2nd, Liang S, Cummins TR (2010) The tarantula toxins ProTx-II and huwentoxin-IV differentially interact with human Nav1.7 voltage sensors to inhibit channel activation and inactivation. *Mol Pharmacol* 78(6):1124–1134.
39. Bosmans F, Martin-Eauclaire MF, Swartz KJ (2008) Deconstructing voltage sensor function and pharmacology in sodium channels. *Nature* 456(7219):202–208.
40. Bosmans F, Puopolo M, Martin-Eauclaire MF, Bean BP, Swartz KJ (2011) Functional properties and toxin pharmacology of a dorsal root ganglion sodium channel viewed through its voltage sensors. *J Gen Physiol* 138(1):59–72.
41. Cox JJ, et al. (2006) An SCN9A channelopathy causes congenital inability to experience pain. *Nature* 444(7121):894–898.
42. Dib-Hajj SD, Black JA, Waxman SG (2009) Voltage-gated sodium channels: therapeutic targets for pain. *Pain Med* 10(7):1260–1269.
43. Drenth JP, Waxman SG (2007) Mutations in sodium-channel gene SCN9A cause a spectrum of human genetic pain disorders. *J Clin Invest* 117(12):3603–3609.
44. Hains BC, et al. (2003) Upregulation of sodium channel Nav1.3 and functional involvement in neuronal hyperexcitability associated with central neuropathic pain after spinal cord injury. *J Neurosci* 23(26):8881–8892.
45. Hains BC, Waxman SG (2007) Sodium channel expression and the molecular pathophysiology of pain after SCI. *Prog Brain Res* 161:195–203.